

MONOCARBOXYLATE TRANSPORTER 1-MEDIATED LACTATE ACCUMULATION PROMOTES NUCLEUS PULPOSUS DEGENERATION UNDER HYPOXIA IN A 3D MULTILAYERED NUCLEUS PULPOSUS DEGENERATION MODEL

C.Y. Wang^{1,2}, M.K. Hsieh^{2,3,5}, Y.J. Hu^{2,3}, A. Bit⁴ and P.L. Lai^{2,3,5,*}

¹International Ph.D. Program in Innovative Technology of Biomedical Engineering and Medical Devices, Ming-Chi University of Technology, No. 84, Gungjuan Road, Taishan District, New Taipei City, 243303, Taiwan

²Bone and Joint Research Centre, Chang Gung Memorial Hospital, No. 5, Fuxing Street, Guishan District, Taoyuan City, 33305, Taiwan

³Department of Orthopaedic Surgery, Chang Gung Memorial Hospital, No. 5, Fuxing Street, Guishan District, Taoyuan City, 33305, Taiwan

⁴Department of Biomedical Engineering, National Institute of Technology, Raipur, 492010, India

⁵College of Medicine, Chang Gung University, No. 259, Wenhua 1st Road, Guishan District, Taoyuan City, 33302, Taiwan

Abstract

During intervertebral disc degeneration (IVDD), due to endplate calcification, diminished oxygen and nutrient concentrations and accumulated lactate are present in the microenvironment of the nucleus pulposus (NP). The disadvantages of 3D layered culture include uneven oxygen and nutrient gradients. In the present study, to mimic the *in vivo* microenvironment of the NP, a 5-layered 3D culture was constructed using clinical haemostatic gelatine sponges and developed as a NP degeneration (NPD) model. Subsequently, cell distribution as well as expression of NP chondrogenic markers (type II collagen and aggrecan), glycosaminoglycan (GAG) and degeneration markers [*e.g.* matrix metalloproteinase (MMP) 3] were measured from the top to the bottom layer. However, in a single NP-cell-loaded disc model, the chondrogenic potency in the middle or bottom layer was higher than that in the top layer. To further study the mechanism underlying the degeneration of NP cells in this NPD model, the contribution of secreted metabolites was examined. Lactate identified in the supernatant modulated GAG accumulation and *MMP3* expression. Inhibition of lactate influx by the monocarboxylate transporter (MCT)-1 inhibitor, AZD3965, reversed the effect of lactate on GAG accumulation and *MMP3* expression and further improved NP cell degeneration in the NPD model. Thanks to the homogenous expression of lactate in the model, it was possible to further identify that the combination of lactate and hypoxia enhanced *MMP3* expression. Taken together, multilayered cell-loaded sponges, with oxygen and nutrient gradients as well as lactate accumulation, can represent a 3D multilayered NPD model for exploring potential agents for IVDD.

Keywords: Nucleus pulposus, 3D cell culture, haemostatic gelatine sponge, degeneration, tissue engineering.

* **Address for correspondence:** Po-Liang Lai, Department of Orthopaedic Surgery, Chang Gung Memorial Hospital, No. 5, Fuxing Street, Guishan District, Taoyuan City, 33305, Taiwan.
Telephone number: +886 33281200 Email: polianglai@gmail.com

Copyright policy: This article is distributed in accordance with Creative Commons Attribution Licence (<http://creativecommons.org/licenses/by/4.0/>).

List of Abbreviations			
2D	two dimensional	AKT	protein kinase B
3D	three dimensional	ATP	adenosine triphosphate
ACAN	aggrecan	AZD	AZD3965
ADAMTSs	ADAM metalloprotease with thrombospondin type 1 motif	CEP	cartilage endplate
AF	annulus fibrosus	COL2A1	type II collagen
		Ct	cycle threshold
		DF	differentiation medium
		DMEM	Dulbecco's modified Eagle medium

DMSO	dimethyl sulphoxide
ECM	extracellular matrix
ERK	extracellular-signal-regulated kinase
FBS	foetal bovine serum
GAG	glycosaminoglycan
GAPDH	glyceraldehyde-3-phosphate dehydrogenase
IVD	intervertebral disc
IVDD	IVD degeneration
MCT	monocarboxylate transporter
MMP	matrix metalloproteinase
MTT	3-(4, 5-dimethylthiazol-2-yl)-2,5-diphenyltetrazoliumbromide
NDRG3	N-Myc downstream-regulated gene family member 3
NP	nucleus pulposus
NPD	NP degeneration
PI3K	phosphoinositide 3-kinase
qRT-PCR	quantitative real-time polymerase chain reaction
Ras	rat sarcoma virus
RGD	Arg-Gly-Asp
SD	standard deviation
SL	single layer
TGF- β 3	transforming growth factor beta 3

Introduction

Low-back pain and neck pain positively correlated with IVDD are experienced by 80 % of the worldwide population and that poses a heavy financial burden on the global healthcare systems (Wáng *et al.*, 2016; Wu *et al.*, 2020). The IVD between two adjacent vertebrae consists of a fibrous ring (AF), a fluid viscoelastic region (NP) and the CEPs, which contribute to spinal mobility and shock absorption. The IVD, a specialised fibrocartilaginous structure, provides flexibility to the spine, allowing limited movements, and supports compressive loads due to body weight and muscle tension (Molladavoodi *et al.*, 2020).

In IVDD, NP degeneration and IVD herniation are two major causes of low-back pain that occur because of the structural impairment of the disc (Yang *et al.*, 2020). Structurally, in ageing IVDs, a fibrous disc with dehydrated NP, loss of disc height, accumulation of granular debris, neovascularisation and increased numbers and sizes of fissures in the peripheral AF have been claimed. Biochemically, aggrecan (the most common proteoglycan in the NP) and type II collagen are the main components of the ECM in the gel-like NP tissue. Three characteristics, including loss of GAGs, an increase in MMP-3 expression, as well as a decrease in COL2A1 and ACAN expression, have been found in NP cells under disc degeneration (Vo *et al.*, 2016). At the beginning of IVDD, the CEP undergoes ossification and thinning, with subsequent microfracture formation, bone sclerosis and reduced perfusion. Subsequently, oxygen and nutrient

supply decrease and cellular wastes and metabolites accumulate in the NP.

In IVDD, the levels of metabolites, including glutamate (Rajasekaran *et al.*, 2021), creatine, glycine, hydroxyproline, alanine, leucine, valine, acetate, isoleucine, alpha- or beta-glucose, myo-inositol (Radek *et al.*, 2016) and lactate (Ohshima and Urban, 1992; Pacholczyk-Sienicka *et al.*, 2015; Radek *et al.*, 2016), are increased in the disc. A high lactate concentration inhibits cell proliferation and decreases collagen II and aggrecan expression in NP cells, which leads to disc degeneration (Shi *et al.*, 2019; Wu *et al.*, 2014). MCT-1 is a major transporter for lactate influx and is expressed ubiquitously in tissues, including NP cells (Silagi *et al.*, 2020). However, it is still unclear if MCT-1 inhibition is beneficial to ECM reconstruction in NP cells.

In addition to the *ex vivo* 3D culture model, many natural and biodegradable biomaterials mixed with hydrogels have been developed as *in vitro* 3D culture models to construct IVDs, such as collagen I, alginate (Moriguchi *et al.*, 2017), chitosan (Roughley *et al.*, 2006; Yuan *et al.*, 2019), silk fibroin, hyaluronan, elastin (Moss *et al.*, 2011) and gelatine (Nagae *et al.*, 2007). In most studies, constructing an IVD tissue is the goal and the bioreactor required for maintaining an IVD tissue needs to provide natural hypoxia and nutrition gradient conditions. Thus, when using a bioreactor, it is hard to observe the cell in a way that would mimic an IVDD. Moreover, immunohistochemistry needs to be performed in tissue sections to assess bioactivities. In some studies, cells are seeded in a SL of materials and the thickness of these materials is less than 10 mm. Culturing cells in a single, thin layer cannot accurately reflect cell behaviour in tissues and the validity of the data obtained are limited when applied to tissue engineering.

A multilayered 3D cell culture system that employs stacked materials, such as chromatographic cellulose papers (Derda *et al.*, 2009; 2011), has been developed. This system is popular because each layer of the 3D stack can easily be isolated and analysed to reveal further biological information, including cell distribution, cell proliferation and gene expression. However, uneven oxygen and nutrient gradients limit the further application of 3D layered cultures (Derda *et al.*, 2011). Interestingly, these disadvantages may mimic the IVDD pathogenesis, which occurs along with endplate ossification and gradual loss of oxygen and nutrients in the IVD microenvironment, indicating the potential of 3D layered cultures to be used as an NPD model. Thus, this 3D multilayered culture model was adapted to establish an IVDD model. However, because the cell morphology and cell proliferation rate would be changed on filter paper relative to cell morphology in the tissue and cell proliferation on the dish culture, cellulose paper may not be a suitable cell culture scaffold (Kuo *et al.*, 2016). Thus, the present study considered the future clinical application and opted for a material that would

accelerate translation. A gelatine-based haemostatic Spongostan™ sponge, a clinically available porous biomaterial with good biocompatibility, was chosen as the culture scaffold for NP cells (Yang *et al.*, 2005).

The study hypothesis was that the microenvironment established by a 3D multilayered culture model could be used to mimic NP degeneration and investigate its pathogenic mechanism. The objective of the study was to establish a multilayered 3D *in vitro* culture model to mimic the pathological condition of NPD. First, GAG accumulation and expression of *COL2A1*, *ACAN* and *MMP3* in each layer were defined. Then, the possible mechanism in the microenvironment that causes degeneration was measured and assessed. Furthermore, a potential agent for improving NPD was evaluated using this 3D *in vitro* NPD model.

Materials and Methods

Bovine caudal IVD dissection, NP cell isolation, culture conditions and reagents for cell treatment

Bovine NP cells were harvested under sterile conditions from the NP tissue in the caudal disc segments of freshly slaughtered calves (4-5 years old) that were obtained from an abattoir (Ching-Chen International Beef store, Taipei, Taiwan) within 24 h of slaughter. The NP tissue was dissected aseptically from the spines of 3 calves ($N = 3$) and the cells were isolated from the tissue through enzymatic digestion using collagenase 2 (2,700 units/10 mL, Gibco) for 16 h at 37 °C. After digestion, the cells were strained using a 40 µm strainer. Then, they were cultured in complete medium [high-glucose DMEM (Gibco) + 10 % FBS (Gibco) + 1 % penicillin/streptomycin (Gibco)] under standard culture conditions (5 % CO₂ and 37 °C) until confluence. 3 NP primary cell cultures were established from each of the 3 calves and cells were expanded (P2-P5) in the complete medium before encapsulation in a 3D gelatine sponge. The 3 bovine NP cell cultures were considered as 3 individual experiments. Cells were induced to undergo chondrogenic differentiation using 2 mL of chondrogenic DF [containing 1 % ITS™ (Sigma-Aldrich), 100 µM sodium pyruvate (Life Technologies), 10 ng/mL TGF-β3 (100-36E, Peprotech), 100 nmol/L dexamethasone (Sigma-Aldrich), 50 µg/mL magnesium L-ascorbic acid-phosphate (Sigma-Aldrich)] for 5-10 d. Medium was replenished every 2-3 d. CoCl₂ (C8661, Sigma-Aldrich), L-lactic acid (L1750, Sigma-Aldrich) and the lactate transporter MCT-1 inhibitor, AZD3965 (AZD, BA164976, Carbosynth, Berkshire, UK), were dissolved in ddH₂O.

Manipulation of the sponge disc and construction of the 3D multilayered model

8 mm diameter and 1 mm thick gelatine sponge (Spongostan™, Johnson & Johnson) discs were prepared using a puncher (provide details). For sterilisation, the discs were immersed in 70 %

ethanol for 15 min and, then, rinsed in 1× PBS 3 times (1 min/time) before being soaked in complete medium overnight. After soaking, the dimensions of the sponge disc reached approximately 8 mm diameter and 2.5 mm thickness. Soft gelatine sponges were prepared for seeding cells. To create a 3D multilayered structure for IVD tissue engineering, 5×10^5 NP cells were seeded directly onto a gelatine sponge in each well of a 24-well plate to mimic the *in vivo* cell density (4,000 cells/mm³) in the NP (Maroudas *et al.*, 1975). Following, cell-seeded sponge discs were placed into an incubator for 2 h at 37 °C, 5 % CO₂. After incubation, 500 µL of complete medium was added to the well overnight. Then, 5 discs (L1-L5) were layered in a stack, placed in a well of a 24-well culture plate and incubated with 2 mL culture medium or chondrogenic DF for 10 d. The SL disc with 5×10^5 NP cells in a well of a 24-well culture plate was also incubated with 2 mL culture medium. The medium was changed every 2-3 d.

Cell viability assay

After single or layered discs had been incubated for 10 d, each NP-cell-seeded gelatine sponge was separated, placed in a well of a 24-well plate and incubated for 1 h at 37 °C in 500 µL of culture medium containing 50 µL of 5 mg/mL MTT reagent (Sigma-Aldrich). Then, MTT solution was discarded and gelatine sponges were washed twice with 1× PBS. The purple products (formazan) of the MTT were dissolved using DMSO (Sigma) and quantified by reading the absorbance at 570 nm using a microplate reader (SpectraMax, M5 Molecular Devices). A sponge without cells was used as a blank for the MTT assay.

Alcian blue staining

Proteoglycan, such as GAGs, secreted by NP cells was stained using alcian blue as described previously (Chen *et al.*, 2018; Woods *et al.*, 2005). Cells were fixed in 4 % paraformaldehyde in 1× PBS for 30 min and washed twice with 1× PBS. Then, cells were rinsed using 3 % acetic acid wash buffer, stained with 1 % alcian blue 8GX (Sigma-Aldrich) for 30 min, de-stained for 10 min in 3 % acetic acid washing solution and washed twice with ddH₂O, until the blank was clear. Alcian-blue-stained GAGs were dissolved in 6 mol/L guanidine hydrochloride (Sigma-Aldrich) overnight at 4 °C. The absorbance of the dissolved and stained GAGs was quantified using a spectrophotometer (SpectraMax M5, Molecular Devices) at optical density 620 nm. A sponge without cells was used as a blank for the alcian blue staining.

Gene expression analysis

qRT-PCR was used to evaluate the RNA level of NP-related gene expressions. NP cells were harvested at the indicated time points and total RNA was extracted using TRIzol™ reagent (Invitrogen). RNA quality and quantity were measured using a Nanodrop™ spectrophotometer (Nanodrop Technologies). Reverse transcription was performed

Table 1. Primer sequences for qRT-PCR. F: forward. R: reverse.

Species	Gene	F or R	Sequence
<i>Bos taurus</i>	COL2A1	F	GGTGGAGCAGCAAGAGCAAG
<i>Bos taurus</i>	COL2A1	R	TTGGGAGCCAGGTTGTCATC
<i>Bos taurus</i>	ACAN	F	TCGGGGGTAGAAGTGTTCATCAGTC
<i>Bos taurus</i>	ACAN	R	ATGGAAGGTGGAGGTGGTTTCAC
<i>Bos taurus</i>	MMP3	F	TCCCCAGTTTCCCCTAATG
<i>Bos taurus</i>	MMP3	R	GGATTCTCCCCTCAGTGTGC
<i>Bos taurus</i>	GAPDH	F	GGTGAAGGTCGGAGTGAACGG
<i>Bos taurus</i>	GAPDH	R	TGCCGTGGGTGGAATCATACTG

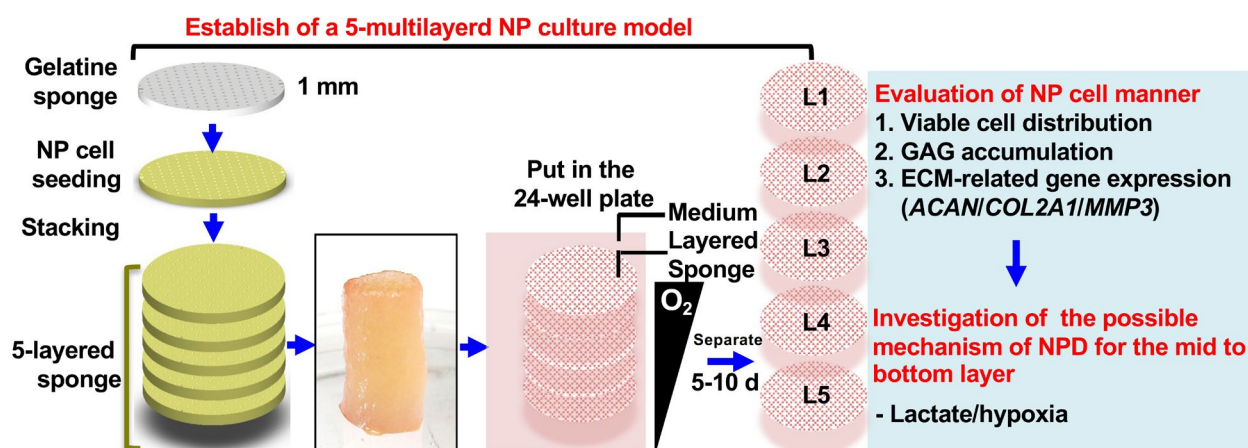


Fig. 1. Schematic representation of the steps for studying a 5-multilayered NPD system. First, after NP cells were seeded in each gelatine disc, the discs were incubated overnight. Then, a 5-multilayered NP cell culture was established in a 24-well plate. The cells loaded on the discs were incubated for 5-10 d after the culture medium was changed to a chondrogenic DF. At the indicated time points, the discs were separated, and NP cell properties were evaluated. Then, the mechanism underlying NPD of the cells in the middle to bottom layers was investigated.

using PrimeScript RT Master Mix (RR036; Takara, Kusatsu, Japan). Then, the cDNA was subjected to qRT-PCR reactions for the quantification of the mRNA levels of *GAPDH*, *SOX-9*, *COL2A1* and *ACAN* using the Power SYBR green PCR Master Mix (4367659; Applied Biosystems). Primer sequences were designed using the Primer 3 system and are listed in Table 1. qRT-PCR analysis was performed using the 96-well QuantStudio5 System (Applied Biosystems). A typical qRT-PCR protocol was performed under the following conditions: 95 °C for 5 min, followed by 40 cycles of denaturation at 95 °C for 15 s and annealing at 60 °C for 60 s. RNA expression of the target gene was normalised first to that of the housekeeping *GAPDH* and then to the indicated control. The $\Delta\Delta C_t$ was used to calculate the relative fold changes. Relative quantification was performed using the comparative CT ($2^{-\Delta\Delta C_t}$) method (Li *et al.*, 2017).

Lactate quantification

Quantification of lactate was performed using a lactate colorimetric assay kit (MAK064, Sigma) according to the manufacturer's protocol. For the quantification of secreted lactate, after the supernatant was centrifuged through a 10 kDa spin

filter, the eluent was diluted 500-fold using the assay buffer and then an assay kit was used to determine the concentration of lactate. For the quantification of the intracellular lactate levels, after sponges were washed twice with 1× PBS, the cells within sponges were lysed and sonicated using the assay buffer. After sonication, the cell lysates were centrifuged using an Eppendorf centrifuge (5814R) at 13,000 ×g for 20 min. The clear supernatant was applied to a 10 kDa spin filter. Then, the eluent was diluted 40-fold using the assay buffer and then the assay kit was used to determine the concentration of lactate. The total protein concentrations of the cell lysates were determined using the Bradford Protein Assay kit (Bio-Rad) according to the manufacturer's protocol. Data are presented as lactate/protein (μmol/mg).

Statistics

Statistical analysis was performed using the SPSS 20.0 software (SPSS, Inc.). All the experimental data are presented as mean ± SD of 3 individual experiments. The statistical significance was evaluated using one-way ANOVA followed by appropriate Bonferroni *post-hoc* tests. The level of statistical significance was set at $p < 0.05$.

Results

Establishing an *in vitro* IVDD model using a multilayered NP cell culture system

Stacking multiple cell-loaded discs to form a 3D layered stack creates a model with gradients of soluble molecules. Further, de-stacking each disc from the 3D layered stack facilitates the analysis of molecules. In this way, it becomes possible to dissect cells in these complex gradients. To create a 3D layered structure for IVD tissue engineering, five 1 mm-thick layers of gelatine sponge (L1-L5) were stacked, each containing the same density of NP cells (Fig. 1). To evaluate the effect of a 3D multilayered culture on cell viability and chondrogenic differentiation, mitochondrial metabolic activity and chondrogenic differentiation marker expression were assessed after the cells were cultured in the chondrogenic DF for 10 d (Fig. 2). Compared with the SL, the number of viable cells distributed in each layer of the 5-layered stack was

decreased ($p < 0.001$) but the difference was no more than 2-fold (Fig. 2a). The expression of chondrogenic-differentiated markers, *COL2A1* ($p < 0.001$) and *ACAN* ($p < 0.001$), and the accumulation of GAGs ($p < 0.001$), were found to be significantly gradually diminished from L1 to L4. Moreover, the markers' expressions and GAG accumulation in L5 were slightly higher than those in L4 (Fig. 2b-d). However, the expression of the degeneration marker *MMP3* was significantly induced in L2-L5, compared with L1 ($p < 0.001$) (Fig. 2e). A SL disc with NP cells in DF medium was taken as a positive control to induce the expression of the chondrogenic markers *COL2A1* and *ACAN* and the accumulation of GAGs. Moreover, a SL disc in complete medium (only DMEM with 10 % FBS and 1 % penicillin/streptomycin) was used as a negative control. For *MMP3* expression, a SL disc in the DF medium was the negative control, while a SL disc in the complete medium was the positive control.

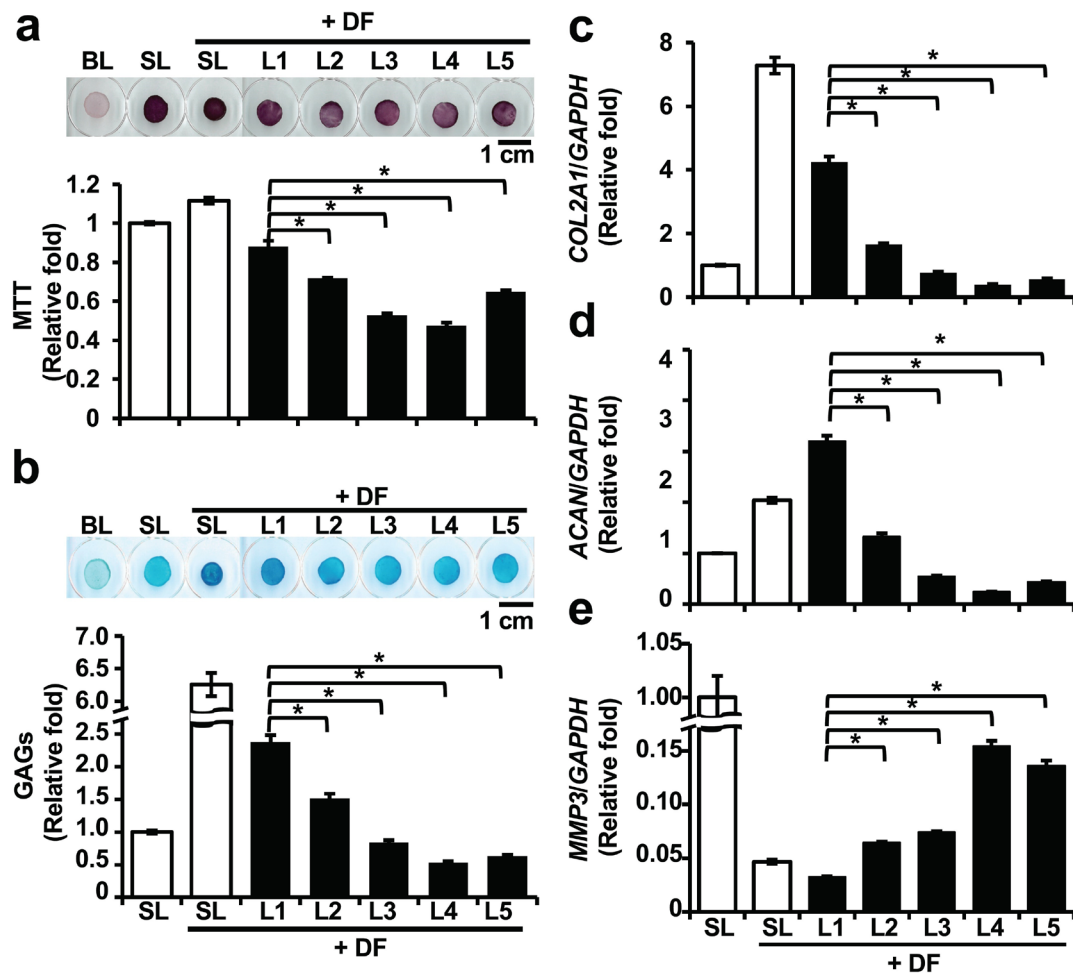


Fig. 2. Properties of the cells in a multilayered sponge 3D culture model. After 10 d incubation of NP cells in a SL or multilayered 3D culture model, (a) the MTT assay was performed to monitor live cell distribution in a SL or from layer 1 to layer 5 (L1-L5). Representative images of discs are presented and the quantitative data are shown. (b) Alcian blue staining was used to determine GAG levels. A representative image of each disc is shown. Scale bar: 1 cm. The relative amount of GAG was quantified by a colorimetric assay. Next, qRT-PCR was performed to determine the expression of chondrogenic-related genes, such as (c) *COL2A1* and (d) *ACAN*, and (e) a degeneration-related gene, such as *MMP3*. The expression of target genes was normalised to that of *GAPDH*. The relative fold change was normalised to the SL without DF medium group. The results are shown as mean \pm SD. $n = 3$, *, $p < 0.001$, compared with L1. BL: blank.

Only the effect of location did not contribute to NP cell degeneration

Derda *et al.* (2011) showed uneven oxygen and nutrient gradients in a 3D layered culture model. To verify the effect of the location in the stack on NP cell degeneration, the disc loaded with NP cells was located on the top layer (L1'), middle layer (L3') or bottom layer (L5') and the other 4 discs did not contain cells. One of the indicators of chondrogenic-like differentiation is GAG accumulation, which is determined by alcian blue staining. Compared with that in L1', the accumulation of GAGs in L3' or L5' was higher ($p < 0.001$) (Fig. 3a,b). The expression of the chondrogenic genes *COL2A1* and *ACAN* in L3' and L5' was upregulated more than that in L1' ($p < 0.001$) (Fig. 3c,d). The expression of *MMP3* was lower in L3' and L5' compared to L1' ($p < 0.001$) (Fig. 3e).

Lactate upregulated *MMP3* expression and downregulated GAG accumulation

Lactate, as a secreted metabolite, accumulates in the degenerated NP tissue (Bartels *et al.*, 1998) and mediates downregulation of GAG, *COL2A1* and *ACAN* expression in a 2D culture model (Wu *et al.*, 2014). To determine the level of lactate released into the supernatant, SL discs or 5-layered sponge discs were cultured in the DF medium for 2 d and, then, the supernatant was harvested and deproteinised using 10 kDa filters. Data showed that the accumulated

concentrations of lactate in SL disc and 5-layered disc cultures were 15 mmol/L and 30 mmol/L, respectively (Fig. 4a).

To understand whether lactate mediated the degeneration of NP cells, NP cells loaded on the sponge discs were treated with lactate at concentrations of 0.5 to 20 mmol/L. The results showed that after treatment for 10 d, the accumulation of GAGs was significantly downregulated in NP cells treated with 20 mmol/L lactate compared with untreated cells cultured in DF medium alone ($p < 0.001$) (Fig. 4b). To investigate whether lactate regulated the expression of chondrogenic-related genes, *MMP3* expression was analysed in NP cells treated with lactate for 1 d (Fig. 4c) or 5 d (Fig. 4d). 10–20 mmol/L lactate significantly induced a 1.6–4.5 fold increase in *MMP3* expression after 5 d but not following 1 d of treatment ($p < 0.001$) (Fig. 4c,d). However, lactate treatment did not significantly affect *ACAN* and *COL2A1* expression (Fig. 4e,f). These data suggested that lactate regulated *MMP3* expression and GAG accumulation but not *ACAN* and *COL2A1* expression.

Inhibition of MCT1-mediated lactate import reversed *MMP3* expression and GAG accumulation

Lactate can be imported into cells through the lactate transporter, MCT-1 (Ritzhaupt *et al.*, 1998). To dissect the mechanism of lactate-mediated GAG accumulation and *MMP3* expression, under

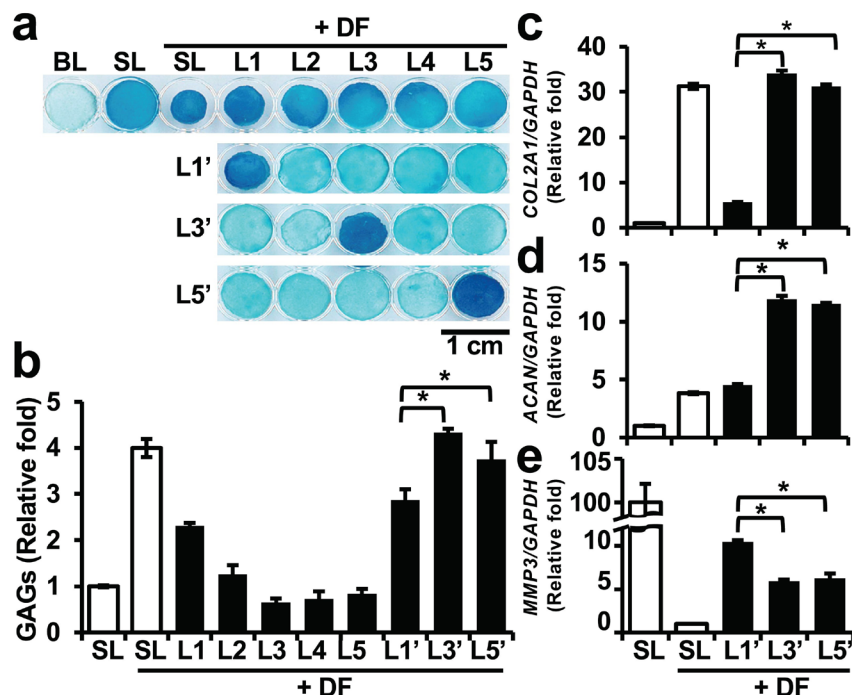


Fig. 3. Effect of sponge location on chondrogenic-like differentiation in the stack. After seeding NP cells in the disc, in addition to the SL culture and a 5-layered culture model, a cell-loaded disc was placed in the top, middle or bottom layer of the stack. After incubation for 10 d, GAG expression was evaluated using alcian blue staining. (a) Representative images of discs are presented. Scale bar: 1 cm. (b) The amount of alcian-blue-stained GAG was eluted using 6 mol/L guanidine hydrochloride and quantified by spectrophotometry. (c-e) qRT-PCR was performed to determine the mRNA levels of *MMP3*, *COL2A1* and *ACAN*. The expression level was normalised to the SL without the DF medium; the results are representative of 3 individual experiments and presented as mean \pm SD. * $p < 0.001$, compared with the L1' group. BL:blank.

SL culture, NP cells were treated with the MCT1 inhibitor AZD (Curtis *et al.*, 2017). As shown in Fig. 4a, lactate was secreted into the supernatant. Thus, half fresh medium mixed with half of the supernatant (from a 5-layered model cultured for 2 d) was used as the source of lactate. This was designated as ½ supernatant. The lactate concentration of ½ supernatant was 10–20 mmol/L. Compared with the ½ supernatant-treated group, the AZD-treated group showed a decrease in intracellular lactate level (Fig. 5a). Without causing cytotoxicity (Fig. 5b), AZD treatment reversed the effect of ½ supernatant on GAG accumulation (Fig. 5c) and *MMP3* expression (Fig. 5d) ($p < 0.001$). Further, cells loaded in a SL sponge disc were pre-treated with AZD overnight. After AZD pre-treatment, the sponges were layered into a 5-layer stack. Following 10 d differentiation, compared with the untreated counterpart, the AZD-treated group of the L3–L5 layers showed significantly lower expression of *MMP3* (Fig. 5e) ($p < 0.001$). These results indicated that in this 3D multilayered model, from the middle to the bottom layer, lactate-regulated

GAG accumulation and *MMP3* expression were MCT1-dependent.

Hypoxia potentiated lactate-induced NP cell degeneration

Given that lactate could induce NP cell degeneration, the next question was whether the distribution of lactate in the 5-layered stack was correlated with the distribution of degenerated NP cells. The lactate concentration in the remaining medium of each destacked disc was determined using a lactate assay. Results revealed that lactate was distributed evenly in the stack (Fig. 6a). To further investigate why the expression of *MMP3* was present as a gradient in the stack, based on the report that an oxygen gradient exists in the stacks (Derda *et al.*, 2009), the hypothesis was that hypoxia potentiated lactate-induced *MMP3* expression. CoCl_2 , a chemical inducer of hypoxia-inducible factor-1, was used to mimic a hypoxic condition. The results showed that lactate or CoCl_2 treatment alone triggered 3–4-fold increases in the expression of *MMP3* compared with the untreated

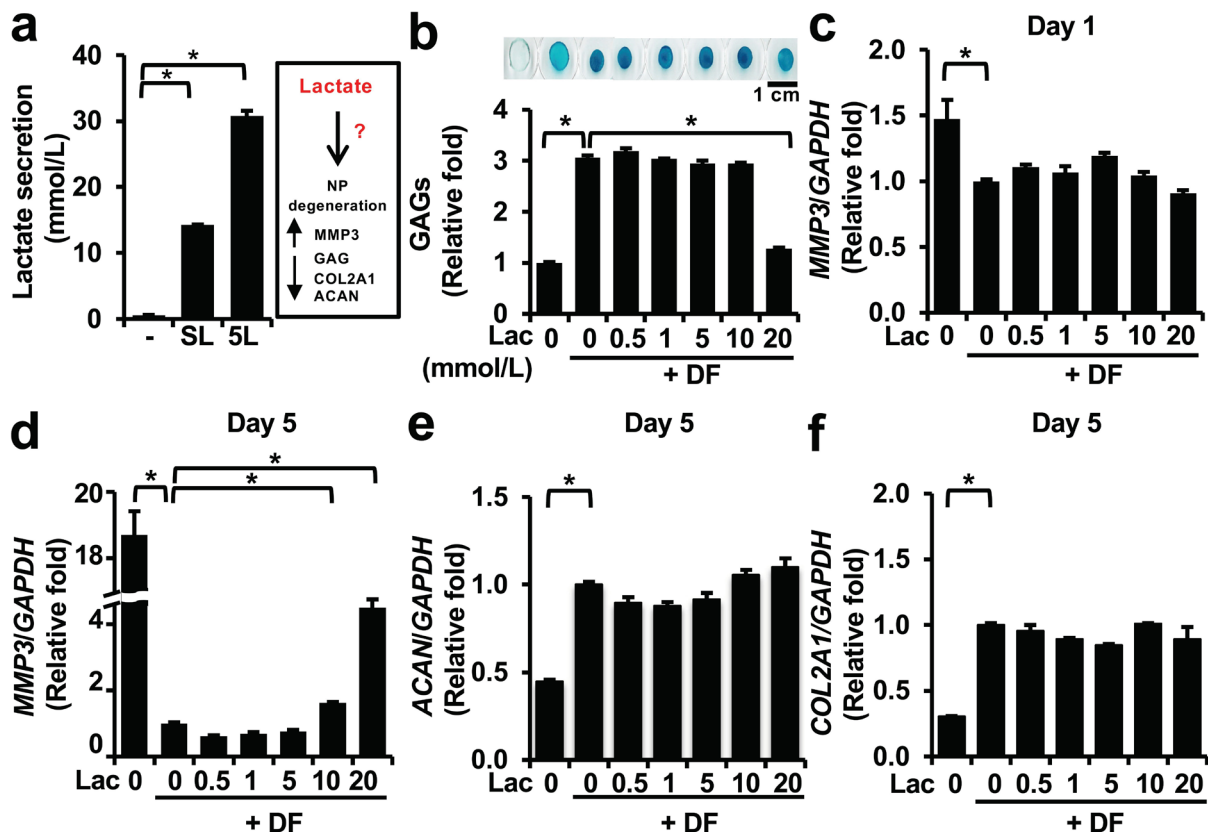


Fig. 4. Lactate was the factor that induced *MMP3* expression and decreased GAG expression. (a) After NP-cells-seeded in a SL or 5-layered (5L) stack were cultured in the DF medium for 2 d, the lactate level in the DF medium was analysed. The results are presented as mean \pm SD. $n = 3$, $* p < 0.001$, compared to day 0 DF medium. (b) NP-cell-loaded sponge discs were cultured in the culture medium or DF medium with the indicated lactate concentration. GAG expression was determined by alcian blue staining after treatment for 10 d. Representative images of discs are presented. Scale bar: 1 cm. The relative level of GAG in the indicated group was normalised to that in the untreated group cultured with the medium alone. After (c) 1 or (d–f) 5 d of the indicated treatment, the mRNA levels of *MMP3*, *ACAN* and *COL2A1* were determined by qRT-PCR and normalised to the levels of *GAPDH*. The relative fold change in target gene expression was normalised to the untreated group cultured with the DF medium. The results are presented as mean \pm SD. $n = 3$, $* p < 0.001$, compared to the untreated group with DF medium.

group. Significantly, combined treatment with lactate and CoCl_2 induced an 8-fold increase in *MMP3* expression (Fig. 6b, $p < 0.001$). These data implied that combined treatment with lactate and hypoxia enhanced NP cell degeneration.

Discussion

Previous studies have shown that gradients of oxygen and nutrient concentrations exist within a 3D multilayered culture, similar to the microenvironmental changes observed during NP degeneration (Bettahalli *et al.*, 2014; Derda *et al.*, 2009; Wang *et al.*, 2019). It has not been shown whether the 3D multilayered culture model can mimic the progress of NPD. The present study hypothesised that NP cells undergo degeneration, which is associated with a gradient of oxygen and nutrient concentrations in a 3D multilayered culture. An *in vitro* NP degeneration model was successfully established, with a gradient of decreased NP-associated ECM gene expression and increased

MMP3 expression from the top to the bottom layer. In this model, MCT-1-mediated lactate influx regulated GAG accumulation and *MMP3* expression. Treatment with MCT-1 inhibitor AZD3965 reversed the lactate-mediated GAG accumulation and *MMP3* expression and alleviated the NP cell degeneration in the 3D layered culture. Furthermore, a combination of lactate and hypoxia enhanced the expression of *MMP3*, suggesting that upregulation of *MMP3* expression in the bottom layer resulted from the effect of low oxygen and lactate concentrations. Consequently, a multilayered 3D culture with oxygen and nutrient gradients could be used as a 3D *in vitro* NPD model to test agents that can improve the IVDD.

To construct a 3D *in vitro* IVDD model, gelatine was chosen as the cell scaffold for the following reasons.

1. The gelatine sponge has the best capacity to keep IVD integrity, compared to tissue glue, polymethyl methacrylate bone cement and platinum oil (Wang *et al.*, 2007).
2. Gelatine is a hydrolysed collagen or denatured collagen, which is composed of

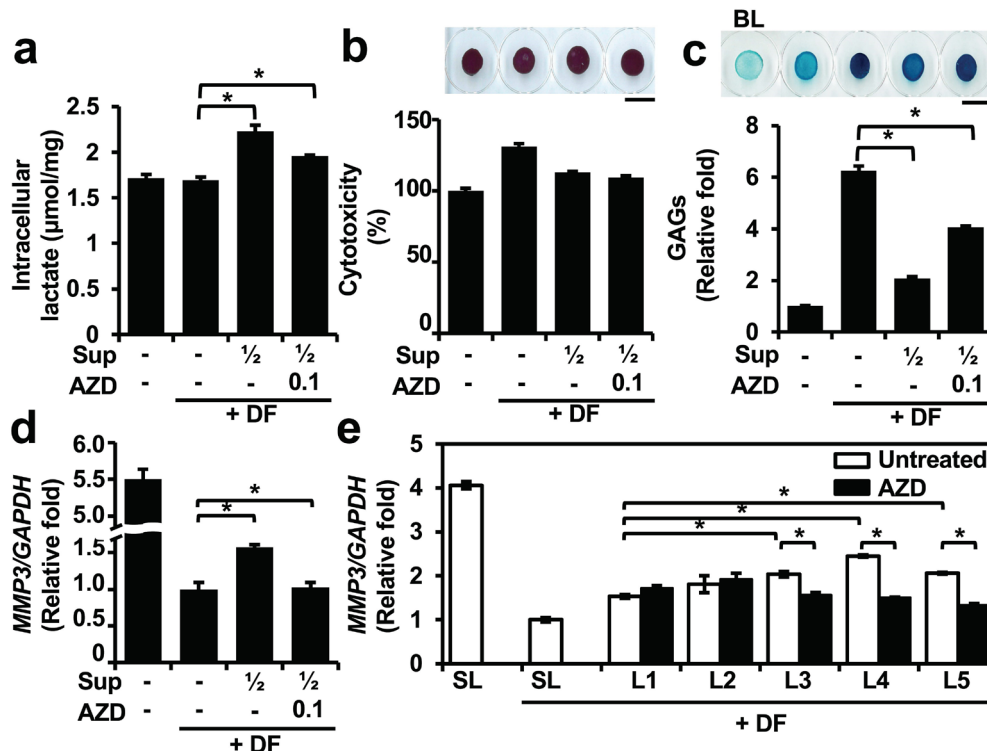


Fig. 5. Inhibition of lactate transport into the cell reversed lactate-induced NP degeneration. NP cells on the SL sponge discs were treated with $\frac{1}{2}$ supernatant (sup) with or without AZD (0.1 $\mu\text{mol/L}$) in the DF medium for 10 d. (a) The intracellular lactate level was measured by lactate colorimetric assay. The level of lactate was normalised to the protein concentration ($\mu\text{mol/mg}$ protein). (b) The cytotoxicity of AZD on the NP cells was detected by MTT assay. The percentage change in cytotoxicity was normalised to that in the untreated group without the DF medium. Scale bar: 1 cm. (c) Alcian blue staining was performed to analyse the GAG content. The relative level of GAG was normalised to that in the untreated group without the DF medium. BL: blank. Scale bar: 1 cm. (d) The mRNA expression of *MMP3* was determined by qRT-PCR. The relative fold change in *MMP3* expression was normalised to that in the untreated group cultured with the DF medium. (e) NP-cell-loaded sponge discs cultured under the 5-layered (L1-L5) conditions were treated with or without AZD for 10 d. The discs in the SL condition treated with DF medium or not were used as positive or negative controls for the *MMP3* expression, respectively. The relative fold change in *MMP3* expression was normalised to that in the untreated group cultured with the DF medium. Results are presented as mean

- proline, hydroxyproline and glycine. Proline and glycine are the basic materials for type II collagen synthesis in NP cells.
- The gelatine sponge used in the present study degrades slowly; thus, it becomes a stage-release agent for releasing proline and glycine (Kuo *et al.*, 2016).
 - Gelatine, with the exposed RGD binding domains, interacts with a specific integrin family transmembrane protein on the cell membrane more strongly and easily than the native form of collagen (Van Agthoven *et al.*, 2014).
 - The pore size of the gelatine sponge used is $148 \pm 62 \mu\text{m}$ (Kuo *et al.*, 2016), which provides a sufficiently large porous structure for cell penetration and attachment.
 - The pore size and the 95 % water content potentially make the gelatine sponge a good biomaterial that allows for the penetration of culture medium containing oxygen and nutrients (Tabata *et al.*, 1999).
 - Considering future clinical applications and for accelerating translation, the present study chose a gelatine-based haemostatic Spongostan™, a clinically available porous biomaterial with good biocompatibility, sponge as the culture scaffold for NP cells (Yang *et al.*, 2005).

In the present study, NP cells were seeded in a gelatine sponge and then a 3D stack was made with multiple cell-loaded sponges. A gel-like cylinder was formed after this 3D stack was cultured for 10 d. The discs were filled with ECM secreted by the NP cells and slightly adhered together. Thus, each layer needed to be separated using a slight force. Once the disc was filled with the ECM, the porosity was reduced as well as the diffusion rates of nutrients,

waste and oxygen. However, in the stack containing only one cell-loaded disc, the ECM just filled in the cell-loaded disc but not the other discs without cells. Compared to those in the 3D stack with only one cell-loaded layer, the low diffusion of nutrients, the gradient of oxygen and even the accumulation of cellular waste, such as lactate, were only observed in the stack with multiple cell-loaded layers. In this multilayered 3D stack, lactate downregulated the expression of *COL2A1* and *ACAN* and accumulation of GAGs but upregulated the expression of *MMP3* along with the nutrient and oxygen concentration gradient. Thus, this 3D multilayered culture could mimic the progress of NPD, in which cells gradually lose nutrient and oxygen support but accumulate lactate in their microenvironment.

Comparing the lactate concentration required to trigger NP cell degeneration in the 2D model to that required in the 3D *in vitro* model, Cs-Szabo *et al.* (2002) showed that in a 2D culture model, a lactate concentration of 2-6 mmol/L is enough to induce NP cell apoptosis and autophagy as well as matrix downregulation. Although findings from the present 3D multilayered model suggested that lactate treatment could directly induce NP cell degeneration, the concentration of lactate that upregulated *MMP3* expression and downregulated GAG accumulation upon 3D culture was 10-20 mmol/L, which was a higher dose of lactate than that required in 2D culture and was more similar to that observed in IVDD patients with relatively low oxygen (Bartels *et al.*, 1998). Accordingly, 3D culture can imitate the *in vivo* environment more accurately than 2D culture.

Facilitating the diffusion of essential nutrients and oxygen to promote cell survival in 3D tissue culturing is possible in scaffolds with pores larger than $100 \mu\text{m}$ (Rouwkema *et al.*, 2008). In the present study, the pore size of the scaffold, a clinically available gelatine

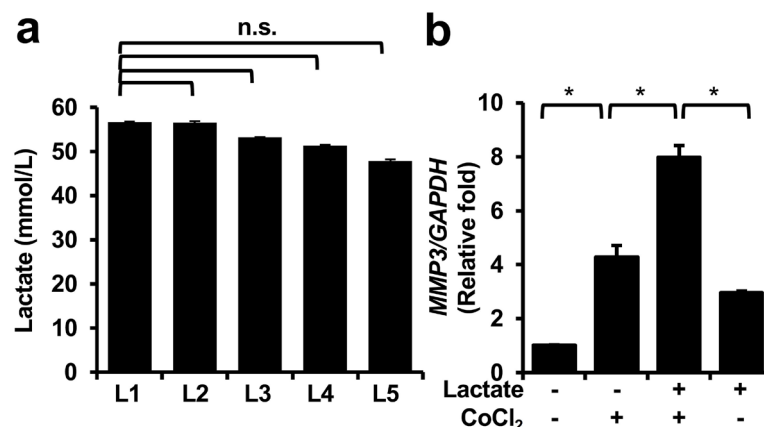


Fig. 6. Lactate and hypoxia had a synergistic effect on *MMP3* expression. (a) After NP cells were cultured on the gelatine sponge with a chondrogenic DF for 10 d, the NP-cell-cultured medium within the gelatine sponge was eluted from each layer. The lactate level in the eluted medium was determined using a lactate assay kit. Results are presented as mean \pm SD. $n = 3$, n.s. = not significant, $p > 0.05$. (b) NP cells were seeded on a gelatine sponge and incubated overnight. Then, CoCl_2 (25 mmol/L) or lactate (20 mmol/L) was applied to the NP cells in a DF medium for 5 d. On day 5, the cells were harvested and the expression of *MMP3* and *GAPDH* was analysed using qRT-PCR. The relative fold change in *MMP3* expression was normalised to the untreated group. Results are presented as mean \pm SD. $n = 3$, * $p < 0.001$.

sponge, was $148 \pm 62 \mu\text{m}$ (Kuo *et al.*, 2016), which is large enough for nutrient and oxygen diffusion. Regarding thickness, the diffusion distance of oxygen and nutrients from vessels to tissues is within $200 \mu\text{m}$ (Jain *et al.*, 2005). Since a single scaffold (1 mm) is not thin enough for nutrient and oxygen diffusion, after multilayered construction, an oxygen gradient within a 5-layered gelatine sponge was obviously formed and cell behaviours (including cell viability and gene expression profile) were changed inside the construct. In a previous study, aerobic pre-osteoblast cells cultured on the bottom layer migrated to the top layer (Wang *et al.*, 2019). However, low-oxygen-requiring NP cells would migrate to the bottom layer (data not shown). The expression of chondrogenic genes, *COL2A1* and *ACAN*, and GAG accumulation in the middle or bottom SL were much greater than that in the top layer. Accordingly, the microenvironment of the bottom layer might represent a better condition for NP cell chondrogenic differentiation than the top layer. This information may be applied to IVD tissue engineering to save the expense of a hypoxia chamber-related equipment.

Lactate, whose concentration gradually increases along with the reduction in oxygen concentration (Ishihara and Urban, 1999), seems to be a potential soluble factor that induces IVDD. The accumulation of lactate and the loss of oxygen diffusion have been observed in IVDD (Ohshima and Urban, 1992). Lactate production and glucose uptake are also augmented under treatment with the hypoxia-inducing agent CoCl_2 (Hwang and Ismail-Beigi, 2002). In the centre of the disc of patients with back pain, the level of lactate produced by anaerobic glycolysis is 10 times higher than that in the plasma (Bartels *et al.*, 1998; Bibby *et al.*, 2005; Ohshima and Urban, 1992). Data in the 3D multilayered NPD model also suggested that NPD occurred in the middle to bottom layers with low oxygen levels. Thus, it was evidenced that low oxygen levels could potentially increase the production of lactate in the cells.

In addition to the level of lactate, hypoxia strengthens the effect of lactate on NP cell degeneration. Data showed that in a CoCl_2 -mimic hypoxic environment, lactate enhanced the expression of IVDD markers, such as *MMP3*. This evidence indicated that the effect of lactate on NP cell degeneration was strengthened under hypoxic conditions, which was not previously investigated. The possible mechanism for lactate-induced NP cell degeneration under hypoxic conditions was proposed as follows. It has been shown that cancer cells may escape lactate-mediated autophagy or apoptosis under hypoxic conditions through an NDRG3-dependent pathway, such as Ras/Erk (Lee *et al.*, 2015) or PI3K/Akt pathways (Liu *et al.*, 2018). However, NDRG3 is an oncogene (Jing *et al.*, 2018), suggesting that NDRG3 may be expressed at a low level or not at all in normal cells, such as NP cells. NP cells may have low NDRG3 expression even under hypoxic conditions, making them more sensitive

to lactate-induced degeneration. Thus, NDRG3 downregulation might be the possible mechanism for lactate-enhanced NP cell degeneration under hypoxic conditions.

Excess lactate in the microenvironment is associated with ECM depletion (Shi *et al.*, 2019). Generally, IVDD is a consequence of the destruction of the ECM. Increased expression of major catabolic enzymes in the ECM, such as *MMP3* and *ADAMTSs*, has been observed in IVDD (Vo *et al.*, 2013). However, it is unclear if excess lactate levels in the microenvironment can regulate the expression of *MMPs*. In the present study, lactate treatment led to the downregulation of sulphated GAG accumulation and the upregulation of *MMP3* expression; however, lactate did not affect the mRNA expression of the ECM-related genes *COL2A1* and *ACAN*. Thus, it is reasonable to conclude that lactate downregulated sulphated GAG accumulation through the upregulation of *MMP3* expression.

MCT is a major lactate transporter. Generally, MCT-1 is a bidirectional lactate transporter and MCT-4 is responsible for lactate export. Silagi *et al.* (2020) demonstrated that MCT-1 and MCT-4 are expressed in NP tissue by using immunohistochemistry staining. In mid to severe grade IVD degeneration (grade 4 to over 7), the percentage of cells expressing MCT-4 was significantly decreased compared to that in the healthy IVD; however, MCT-1 expression was persistent. Thus, the role of MCT-1 cannot be neglected. It is still unclear if MCT-1 inhibition is beneficial for the reconstruction of the ECM by NP cells. The present results demonstrated that AZD3965, an MCT1-specific inhibitor, significantly reduced lactate influx and decreased *MMP3* expression even under low oxygen conditions. Although AZD3965 is a preclinical drug for adult solid cancer treatment, it may have potential for improving IVDD. Thus, in the future, AZD3965 may be applied to the affected spinal region and used as an early-stage IVDD treatment.

Conclusion

The present study successfully established a 3D multi-layered *in vitro* NPD model. In this model, the expression of the degeneration marker *MMP3* and the chondrogenic markers *COL2A1* and *ACAN* as well as the accumulation of GAGs were observed as a gradient in the stack. The inhibition of oxygen and nutrient diffusion as well as the accumulation of the metabolite lactate were identified as degeneration factors. Furthermore, lactate influx induced *MMP3* expression as a potential mechanism underlying NPD; however, using AZD3965 to inhibit MCT1 limited the lactate influx and improved NPD. Moreover, under a hypoxic condition, lactate dramatically enhanced *MMP3* expression. Overall, the oxygen gradient in the 3D multilayered NPD model modulated the disc degeneration in response to lactate. This construct has the potential to be used for studying therapeutic

agents of NPD and the knowledge from the present study may be applied to NPD treatment and NP tissue engineering.

Acknowledgements

This study was supported by a grant (VK000-1G00-110) from the Ming Chi University of Technology, a grant (CMRPG3K1041, CMRPG3K1042) from the Linkou Chang Gung Memorial Hospital, Taiwan and grants (109-2221-E-182A-002, 107-2923-B-182A-001-MY3) from the Ministry of Science and Technology, Taiwan. We appreciate the equipment support from the Clinical Proteomics Core Laboratory in Chang Gung Memorial Hospital, Linkou, Taiwan.

References

- Bartels EM, Fairbank JC, Winlove CP, Urban JP (1998) Oxygen and lactate concentrations measured *in vivo* in the intervertebral discs of patients with scoliosis and back pain. *Spine (Phila Pa 1976)* **23**: 1-8.
- Bettahalli NM, Groen N, Steg H, Unadkat H, de Boer J, van Blitterswijk CA, Wessling M, Stamatialis D (2014) Development of multilayer constructs for tissue engineering. *J Tissue Eng Regen Med* **8**: 106-119.
- Bibby SR, Jones DA, Ripley RM, Urban JP (2005) Metabolism of the intervertebral disc: effects of low levels of oxygen, glucose, and pH on rates of energy metabolism of bovine nucleus pulposus cells. *Spine (Phila Pa 1976)* **30**: 487-496.
- Chen YC, Wu KC, Huang BM, So EC, Wang YK (2018) Midazolam inhibits chondrogenesis *via* peripheral benzodiazepine receptor in human mesenchymal stem cells. *J Cell Mol Med* **22**: 2896-2907.
- Cs-Szabo G, Ragasa-San Juan D, Turumella V, Masuda K, Thonar EJ, An HS (2002) Changes in mRNA and protein levels of proteoglycans of the annulus fibrosus and nucleus pulposus during intervertebral disc degeneration. *Spine (Phila Pa 1976)* **27**: 2212-2219.
- Curtis NJ, Mooney L, Hopcroft L, Michopoulos F, Whalley N, Zhong H, Murray C, Logie A, Revill M, Byth KF, Benjamin AD, Firth MA, Green S, Smith PD, Critchlow SE (2017) Pre-clinical pharmacology of AZD3965, a selective inhibitor of MCT1: DLBCL, NHL and Burkitt's lymphoma anti-tumor activity. *Oncotarget* **8**: 69219-69236.
- Derda R, Laromaine A, Mammoto A, Tang SK, Mammoto T, Ingber DE, Whitesides GM (2009) Paper-supported 3D cell culture for tissue-based bioassays. *Proc Natl Acad Sci U S A* **106**: 18457-18462.
- Derda R, Tang SK, Laromaine A, Mosadegh B, Hong E, Mwangi M, Mammoto A, Ingber DE, Whitesides GM (2011) Multizone paper platform for 3D cell cultures. *PLoS One* **6**: e18940. DOI: 10.1371/journal.pone.0018940.
- Hwang DY, Ismail-Beigi F (2002) Glucose uptake and lactate production in cells exposed to CoCl₂ and in cells overexpressing the Glut-1 glucose transporter. *Arch Biochem Biophys* **399**: 206-211.
- Ishihara H, Urban JP (1999) Effects of low oxygen concentrations and metabolic inhibitors on proteoglycan and protein synthesis rates in the intervertebral disc. *J Orthop Res* **17**: 829-835.
- Jain RK, Au P, Tam J, Duda DG, Fukumura D (2005) Engineering vascularized tissue. *Nat Biotechnol* **23**: 821-823.
- Jing J-S, Li H, Wang S-C, Ma J-M, Yu L-Q, Zhou H (2018) NDRG3 overexpression is associated with a poor prognosis in patients with hepatocellular carcinoma. *Biosci Rep* **38**: BSR20180907. DOI: 10.1042/BSR20180907.
- Kuo ZK, Lai PL, Toh EK, Weng CH, Tseng HW, Chang PZ, Chen CC, Cheng CM (2016) Osteogenic differentiation of preosteoblasts on a hemostatic gelatine sponge. *Sci Rep* **6**: 32884. DOI: 10.1038/srep32884.
- Lee D, Sohn H, Park Z-Y, Oh S, Kang Y, Lee K-M, Kang M, Jang Y, Yang S-J, Hong Y, Noh H, Kim J-A, Kim D, Bae K-H, Kim D, Chung S, Yoo H, Yu D-Y, Park K, Yeom Y (2015) A lactate-induced response to hypoxia. *Cell* **161**: 595-609.
- Li X-C, Tang Y, Wu J-H, Yang P-S, Wang D-L, Ruan D-K (2017) Characteristics and potentials of stem cells derived from human degenerated nucleus pulposus: potential for regeneration of the intervertebral disc. *BMC Musculoskelet Disord* **18**: 242-253.
- Liu Y-P, Xu P, Guo C-X, Luo Z-R, Zhu J, Mou F-F, Cai H, Wang C, Ye X-C, Shao S-J, Guo H-D (2018) miR-1b overexpression suppressed proliferation and migration of RSC96 and increased cell apoptosis. *Neurosci Lett* **687**: 137-145.
- Maroudas A, Stockwell RA, Nachemson A, Urban J (1975) Factors involved in the nutrition of the human lumbar intervertebral disc: cellularity and diffusion of glucose *in vitro*. *J Anat* **120**: 113-130.
- Molladavoodi S, McMorrnan J, Gregory D (2020) Mechanobiology of annulus fibrosus and nucleus pulposus cells in intervertebral discs. *Cell Tissue Res* **379**: 429-444.
- Moriguchi Y, Mojica-Santiago J, Grunert P, Pennicooke B, Berlin C, Khair T, Navarro-Ramirez R, Ricart Arbona RJ, Nguyen J, Hartl R, Bonassar LJ (2017) Total disc replacement using tissue-engineered intervertebral discs in the canine cervical spine. *PLoS One* **12**: e0185716. DOI: 10.1371/journal.pone.0185716.
- Moss IL, Gordon L, Woodhouse KA, Whyne CM, Yee AJ (2011) A novel thiol-modified hyaluronan and elastin-like polypeptide composite material for tissue engineering of the nucleus pulposus of the intervertebral disc. *Spine (Phila Pa 1976)* **36**: 1022-1029.
- Nagae M, Ikeda T, Mikami Y, Hase H, Ozawa H, Matsuda K, Sakamoto H, Tabata Y, Kawata M, Kubo T (2007) Intervertebral disc regeneration using platelet-rich plasma and biodegradable gelatine hydrogel microspheres. *Tissue Eng* **13**: 147-158.

- Ohshima H, Urban JP (1992) The effect of lactate and pH on proteoglycan and protein synthesis rates in the intervertebral disc. *Spine (Phila Pa 1976)* **17**: 1079-1082.
- Pacholczyk-Sienicka B, Radek M, Radek A, Jankowski S (2015) Characterization of metabolites determined by means of 1H HR MAS NMR in intervertebral disc degeneration. *MAGMA* **28**: 173-183.
- Radek M, Pacholczyk-Sienicka B, Jankowski S, Albrecht L, Grodzka M, Depta A, Radek A (2016) Assessing the correlation between the degree of disc degeneration on the Pfirrmann scale and the metabolites identified in HR-MAS NMR spectroscopy. *Magn Reson Imaging* **34**: 376-380.
- Rajasekaran S, Soundararajan DCR, Nayagam SM, Tangavel C, Raveendran M, Thippeswamy PB, Djuric N, Anand SV, Shetty AP, Kanna RM (2021) Modic changes are associated with activation of intense inflammatory and host defense response pathways – molecular insights from proteomic analysis of human intervertebral discs. *Spine J* **22**: 19-38.
- Ritzhaupt A, Wood IS, Ellis A, Hosie KB, Shirazi-Beechey SP (1998) Identification and characterization of a monocarboxylate transporter (MCT1) in pig and human colon: its potential to transport L-lactate as well as butyrate. *J Physiol* **513**: 719-732.
- Roughley P, Hoemann C, DesRosiers E, Mwale F, Antoniou J, Alini M (2006) The potential of chitosan-based gels containing intervertebral disc cells for nucleus pulposus supplementation. *Biomaterials* **27**: 388-396.
- Rouwkema J, Rivron NC, van Blitterswijk CA (2008) Vascularization in tissue engineering. *Trends Biotechnol* **26**: 434-441.
- Shi J, Zhou X, Wang Z, Kurra S, Niu J, Yang H (2019) Increased lactic acid content associated with extracellular matrix depletion in a porcine disc degeneration induced by superficial annular lesion. *BMC Musculoskelet Disord* **20**: 551. DOI: 10.1186/s12891-019-2937-x.
- Silagi ES, Novais EJ, Bisetto S, Telonis AG, Snuggs J, Le Maitre CL, Qiu Y, Kurland IJ, Shapiro IM, Philp NJ, Risbud MV (2020) Lactate efflux from intervertebral disc cells is required for maintenance of spine health. *J Bone Miner Res* **35**: 550-570.
- Tabata Y, Nagano A, Ikada Y (1999) Biodegradation of hydrogel carrier incorporating fibroblast growth factor. *Tissue Eng* **5**: 127-138.
- Van Agthoven JF, Xiong J-P, Alonso JL, Rui X, Adair BD, Goodman SL, Arnaout MA (2014) Structural basis for pure antagonism of integrin $\alpha V\beta 3$ by a high-affinity form of fibronectin. *Nat Struct Mol Biol* **21**: 383-388.
- Vo NV, Hartman RA, Patil PR, Risbud MV, Kletsas D, Iatridis JC, Hoyland JA, Le Maitre CL, Sowa GA, Kang JD (2016) Molecular mechanisms of biological aging in intervertebral discs. *J Orthop Res* **34**: 1289-1306.
- Vo NV, Hartman RA, Yurube T, Jacobs LJ, Sowa GA, Kang JD (2013) Expression and regulation of metalloproteinases and their inhibitors in intervertebral disc aging and degeneration. *Spine J* **13**: 331-341.
- Wang CY, Kuo ZK, Hsieh MK, Ke LY, Chen CC, Cheng CM, Lai PL (2019) Cell migration of preosteoblast cells on a clinical gelatine sponge for 3D bone tissue engineering. *Biomed Mater* **15**: 015005. DOI: 10.1088/1748-605X/ab4fb5.
- Wang YH, Kuo TF, Wang JL (2007) The implantation of non-cell-based materials to prevent the recurrent disc herniation: an *in vivo* porcine model using quantitative discomanometry examination. *Eur Spine J* **16**: 1021-1027.
- Wáng YXJ, Wáng J-Q, Káplár Z (2016) Increased low back pain prevalence in females than in males after menopause age: evidences based on synthetic literature review. *Quant Imaging Med Surg* **6**: 199-206.
- Woods A, Wang G, Beier F (2005) RhoA/ROCK signaling regulates Sox9 expression and actin organization during chondrogenesis. *J Biol Chem* **280**: 11626-11634.
- Wu A, March L, Zheng X, Huang J, Wang X, Zhao J, Blyth FM, Smith E, Buchbinder R, Hoy D (2020) Global low back pain prevalence and years lived with disability from 1990 to 2017: estimates from the Global Burden of Disease Study 2017. *Ann Transl Med* **8**: 299-299.
- Wu W, Zhang X, Hu X, Wang X, Sun L, Zheng X, Jiang L, Ni X, Xu C, Tian N, Zhu S, Xu H (2014) Lactate down-regulates matrix synthesis and promotes apoptosis and autophagy in rat nucleus pulposus cells. *J Orthop Res* **32**: 253-261.
- Yang S, Zhang F, Ma J, Ding W (2020) Intervertebral disc ageing and degeneration: the antiapoptotic effect of oestrogen. *Ageing Res Rev* **57**: 100978. DOI: 10.1016/j.arr.2019.100978.
- Yang SH, Chen PQ, Chen YF, Lin FH (2005) Gelatin/chondroitin-6-sulfate copolymer scaffold for culturing human nucleus pulposus cells *in vitro* with production of extracellular matrix. *J Biomed Mater Res B Appl Biomater* **74**: 488-494.
- Yuan D, Chen Z, Xiang X, Deng S, Liu K, Xiao D, Deng L, Feng G (2019) The establishment and biological assessment of a whole tissue-engineered intervertebral disc with PBST fibers and a chitosan hydrogel *in vitro* and *in vivo*. *J Biomed Mater Res B Appl Biomater* **107**: 2305-2316.

Discussion with Reviewers

Tang Shirley: Can you comment on the differences you might expect to observe if the study was performed on human NP cells instead of bovine cells? **Authors:** We think the results from bovine and human NP cells would be similar. However, human fresh NP tissue is very difficult to obtain while bovine NP tissue it is easily available from slaughterhouses. We have recently purchased human NP cells. Despite that human NP cells are larger than bovine NP cells, their

growth rate is slower than that of bovine NP cells. Thus, it would take longer to get sufficient numbers of cells to perform the experiments.

Reviewer: The authors provided an extensive justification for using gelatine sponges in this multilayered construct. Can they comment on the differences they may expect to observe with other types of commonly used biomaterials for NP repair, e.g. collagen or hyaluronic acid hydrogels?

Authors: If collagen or hyaluronic acid hydrogels is used, stiffness/softness and degradation velocity of the hydrogel need to be a concern. The hydrogel might be too soft to be layered. Moreover, its stiffness may affect cell proliferation rate as well as lactate production levels.

Gay Max: In your AZD rescue model, you pre-treated in SL and then stacked the next day. Have you thought about first performing your degeneration model and then adding the AZD to rescue the degeneration? What would you expect the outcome of such a scenario be?

Authors: The ECM secreted by the NP cells makes the sponge become a gel and decreases the water and mass permeability; therefore, if the degeneration model was set up first and then the AZD drug added, the drug will probably not be very well absorbed into

the discs. This may influence its effect. Thus, the discs were treated before layering. Based on this question, the treatment of AZD was performed following layering. Surprisingly, the effect of AZD after layering was the same as that before layering.

Gay Max: Lactate will accumulate in the medium even if the receptor is blocked. Which effect do you think the change in osmolarity will have on the cells and the model?

Authors: According to Krouwels *et al.* (2018, additional reference), the higher osmolarity of the medium will make NP cells have more ECM. However, in the present model, the medium was changed every 2 d, so as not to affect osmolarity.

Additional Reference

Krouwels A, Melchels FPW, van Rijen MHP, Öner FC, Dhert WJA, Tryfonidou MA, Creemers LB (2018) Comparing hydrogels for human nucleus pulposus regeneration: role of osmolarity during expansion. *Tissue Eng Part C Methods* **24**: 222-232.

Editor's note: The Guest Editor responsible for this paper was Andrea Vernengo.